The response (1958–1997) of permafrost and near-surface ground temperatures to forest fire, Takhini River valley, southern Yukon Territory

C.R. Burn

Abstract: Forest fires in permafrost areas often modify ground surface conditions, causing deepening of the active layer and thawing of near-surface permafrost. Takhini River valley lies in the discontinuous permafrost zone of southern Yukon Territory. The valley floor is covered by glaciolacustrine deposits, which are locally ice rich. In 1958 extensive forest fires burned most of the vegetation and the soil organic horizon in the valley, but, 50 km west of Whitehorse, 1 km^2 of spruce forest adjacent to the Alaska Highway escaped burning. Permafrost beneath this stand of trees is in equilibrium with surface conditions: the active layer is 1.4 m thick, the base of permafrost is at 18.5 m, the annual mean temperature at the top of permafrost (1.5 m) is –0.8°C, and the temperature gradient in permafrost is constant with depth. At burned sites nearby there has been little regeneration of forest vegetation since the fire, and long-term permafrost degradation has occurred. At one burned site, the permafrost table is more than 3.75 m below the ground surface, the mean annual ground temperature is –0.2°C or warmer throughout the profile, the annual mean temperature at 1.5 m is 0.1°C, and permafrost is thawing from top and bottom. A simplified analytical model for thawing of permafrost indicates that over a millennium will be required to degrade permafrost completely at this site, if thawing proceeds from the top down. The result demonstrates the persistence of ice-rich permafrost a few metres below the ground surface, even at sites near the southern margin of permafrost in Canada.

Résumé : Les feux de forêt dans les régions pergélisolées modifient fréquemment les conditions de la surface, causant un approfondissement de la couche active et une fonte de la glace du pergélisol près de la surface. La vallée de la rivière Takhini se situe dans la zone de pergélisol discontinu, dans la région sud du Territoire du Yukon. Le fond de la vallée est couvert de dépôts glaciolacustres, qui incorpore localement de grandes quantités de glace. En 1958, d'importants feux de forêt ont brûlé la majeure partie de la végétation et de l'horizon organique des sols dans la vallée, mais, à 50 km à l'ouest de Whitehorse, une forêt d'épinettes de1 km^2 adjacente à la route de l'Alaska fut protégée des flammes. Sous ce peuplement d'arbres, le pergélisol est en équilibre avec les conditions de surface : la couche active a une épaisseur de 1,4 m, la base du pergélisol est à 18,5 m, la température moyenne annuelle au sommet du pergélisol (1,5 m) est –0,8°C et le gradient de température dans le pergélisol ne varie pas avec la profondeur. Dans les endroits voisins incendiés, il n'y a eu qu'une très faible régénération de la végétation forestière depuis le feu, et une dégradation à long terme du pergélisol a été amorcée. Un site incendié montre que le niveau supérieur du pergélisol se situe maintenant à plus de 3,75 m sous la surface du sol, la température annuelle du sol au travers le profil est –0,2°C ou plus, la température moyenne annuelle à 1,5 m est 0,1°C et il y a dégel du pergélisol au sommet et au fond. Un modèle analytique simplifié de la fonte du pergélisol indique que plus de mille ans seront nécessaires pour complètement dégrader le pergélisol sur ce site, si la fonte progresse du sommet vers le bas. Le résultat démontre la pérennité des niveaux pergélisolés riches en glace à quelque mètres sous la surface du sol, même pour les sites à proximité de la marge méridionale du pergélisol au Canada.

[Traduit par la rédaction]

Introduction

In the discontinuous permafrost zone, four critical microclimatic variables control the presence of perennially frozen ground: the depth of snow cover, the thickness of the soil's organic horizon, the soil moisture content, and the nature of the vegetation canopy (Smith 1975; Williams and Burn 1996). Variation in these surface conditions controls the presence or absence of permafrost more than fluctuations in the climatic regime (Smith and Riseborough 1983). The most widespread changes in surface conditions that cause permafrost degradation in forested areas are wrought by wild fires (Viereck 1982; Zoltai 1993).

The principal alteration to the components of the surface energy balance following fire is a decrease in evapotranspiration, causing an increase in both ground surface temperature and the ground heat flux (Rouse 1976). As a result, forest fires often lead to deepening of the active layer and thawing of near-surface permafrost (Mackay 1977, 1995; Viereck 1982; Zhou et al. 1993). The most pronounced permafrost degradation occurs after intense fires that destroy the surface organic layer: in contrast, active-layer depth may be unaffected in wetlands, where moss and humus may survive the fire (Swanson 1996).

Received June 27, 1997. Accepted November 4, 1997.

C.R. Burn. Department of Geography, and Ottawa–Carleton Centre for Geoscience Studies, Carleton University, 1125 Colonel By Drive, Ottawa, ON K1S 5B6, Canada (e-mail: crburn@ccs.carleton.ca).

Fig. 1. Location map, indicating proximity of study area to Whitehorse, Yukon Territory.

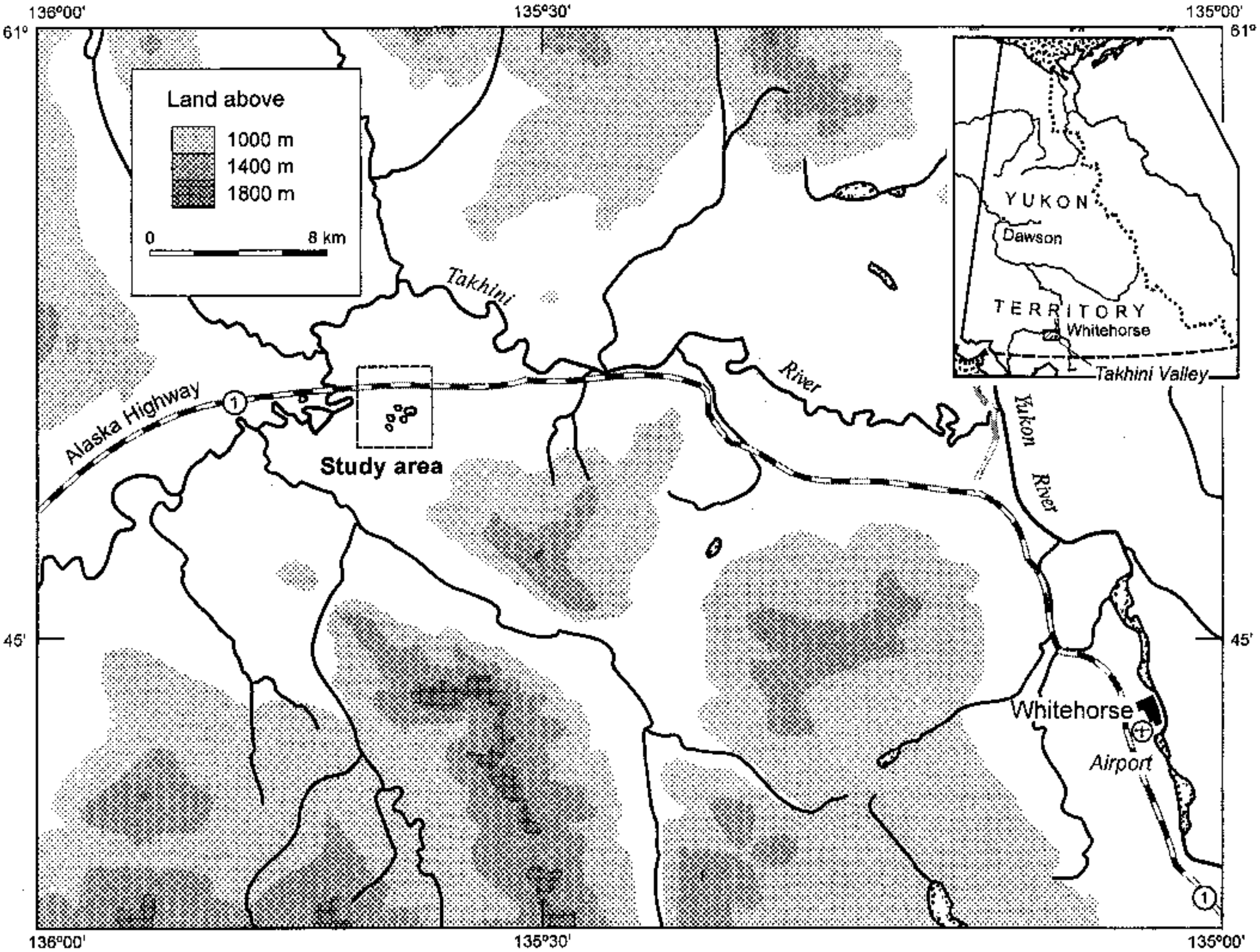

As vegetation regenerates in the years following fire, the surface energy balance approaches that of undisturbed terrain, the antefire active-layer thickness is reestablished, and the ground stabilizes (Viereck 1973; Rouse 1976; Mackay 1995). However, at sites where vegetation regeneration is slow, long-term permafrost degradation may continue. The purpose of this paper is to describe permafrost degradation following an intense forest fire in July 1958, at a site in Takhini River valley, 50 km west of Whitehorse, Yukon Territory (Fig. 1). The thermal regime of permafrost beneath a 1 km^2 unburned stand of spruce trees is compared with ground temperatures beneath a burned site and in a meadow nearby. The paper contributes to understanding the role of fire in northern ecosystems (e.g., Moore 1996), which may increase in practical significance if wild fires become more frequent as a result of climate change (Flannigan and Van Wagner 1991).

Study area

Takhini River valley is a flat valley, 8 km wide, that lies in Yukon Plateaus physiographic unit, separating the tablelands of Lewes Plateau physiographic area from those of Teslin Plateau (Mathews 1986). The region was glaciated during the Late Wisconsinan McConnell advance (Hughes et al. 1989), and most of the valley sides are covered by a veneer of glacial drift. The valley floor is a glaciolacustrine plain, covered by silt and clay interbedded with fine sand (Rampton et al. 1983; Morison and Klassen 1991). Thermokarst lakes and other ponds are clustered in various parts of the valley; most appear on aerial photographs taken before the forest fire (Fig. 2*a*), and some have been stable over millennia (Klassen 1979; Keenan and Cwynar 1992).

The area has a continental climate similar to that of Whitehorse (Table 1), with a short summer and long winter; intensely cold spells occur in winter when a topographically enhanced inversion develops (Wahl et al. 1987). The area is in the rain shadow of the Coast Mountains, and both aridity and the particular severity of the fire are principal reasons for the absence of spruce saplings and the lack of an organic horizon at burned sites 39 years after the fire (K. Kepke, personal communication, 1997). Before the fire, most of the valley was covered by a white spruce forest, which had dominated the vegetation of the region for at least the previous 8 ka (Keenan and Cwynar 1992). Since the fire, the valley floor has been

Fig. 2. Aerial photographs of the study area in Takhini River valley, southern Yukon Territory. The Alaska Highway runs across the photographs from left (west) to right (east). (*a*) 25 August 1946, 12 years before the forest fire. Several thermokarst lakes are visible near the gravel pit and the forest is ubiquitous. (*b*) 12 August 1979, 20 years after the fire, illustrating minimal forest vegetation succession on the valley floor. The three large dots represent the location of thermistor cables at the forest (F), burned (B), and meadow (M) sites; open circles indicate the locations of holes drilled in 1982. The boreholes drilled by Geological Survey of Canada in 1978 were located adjacent to B (Klassen 1979). Parts of aerial photographs A10565-6 ©1946 Her Majesty the Queen in Right of Canada, and A25275-22 ©1979 Her Majesty the Queen in Right of Canada, reproduced from the collection of the National Air Photo Library with permission of Natural Resources Canada.

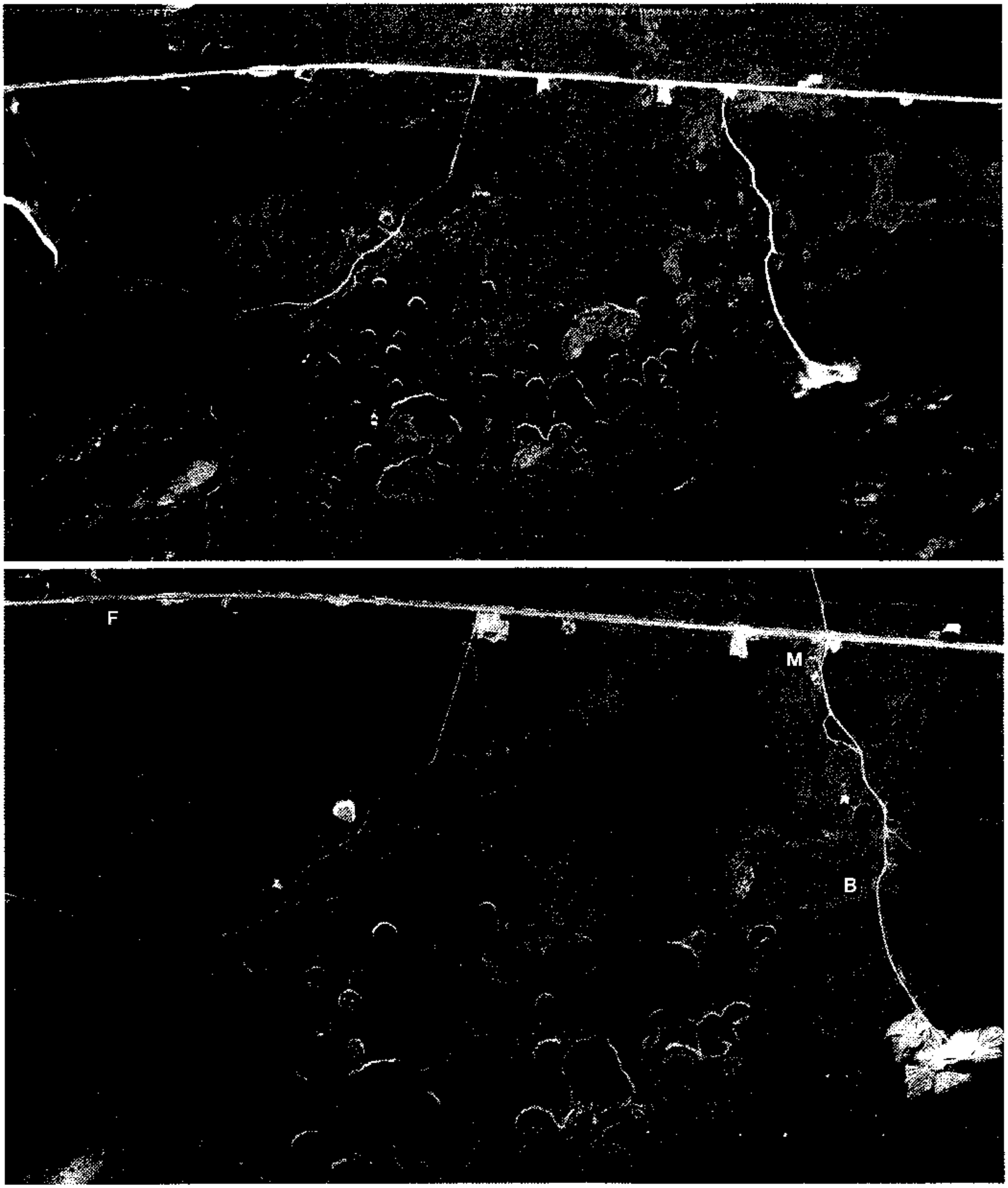

Table 1. Normal climate data for Whitehorse Airport, 1961–1990.

	Jan.	Feb.	Mar.	Apr.	May	June	July	Aug.	Sept.	Oct.	Nov.	Dec.	Year
Daily mean air temperature (°C)	−18.7	−13.1	−7.2	0.3	6.6	11.6	14.0	12.3	7.3	0.7	−10.0	−15.9	−1.0
Total rainfall (mm)	0.2	0.0	0.0	1.0	11.8	30.3	38.5	38.1	30.5	7.6	1.2	0.3	159.6
Total snowfall (cm)	23.0	16.6	16.9	9.8	2.9	0.9	0.0	1.1	4.8	18.7	25.5	25.1	145.2
Month-end snow depth (cm)	34	33	28	3	0	0	0	0	0	4	16	27	

Notes: Environment Canada (1993) is the source for the data in this table.

Fig. 3. Photographs of the ground temperature sites taken in February 1992: (*a*) in the unburned spruce forest; (*b*) in the burned area.

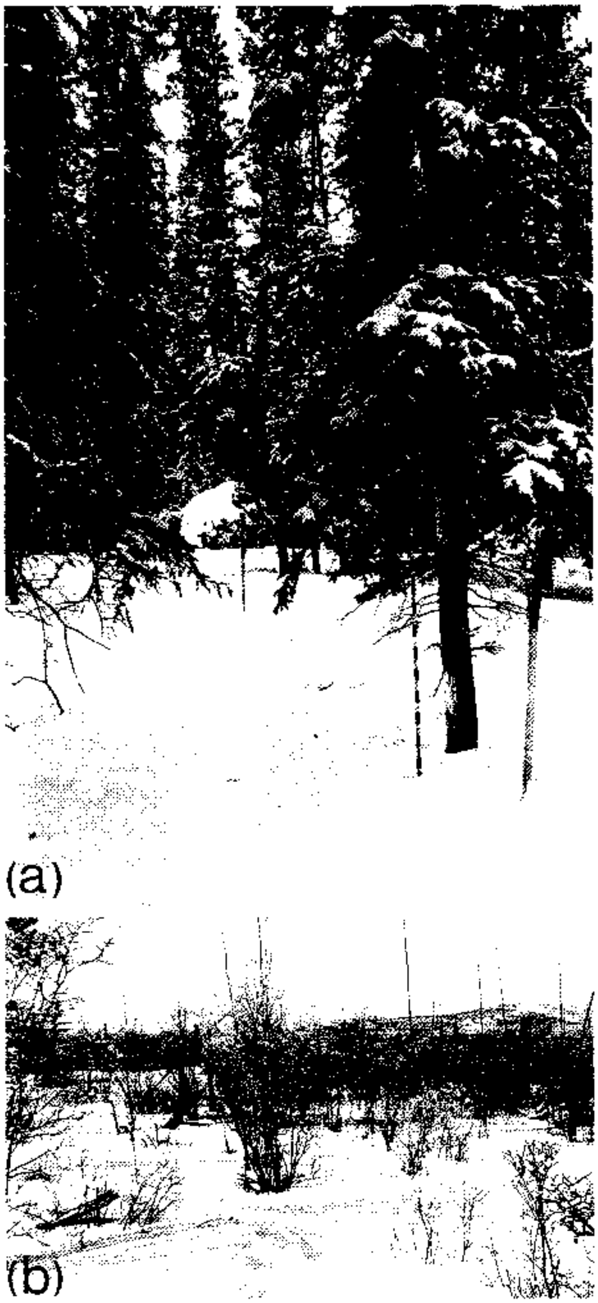

Fig. 4. Installations for monitoring air temperature: (*a*) at the forest site; (*b*) at the burned site. Photographs taken in August 1995.

unevenly colonized by trembling aspen, clumps of willow, a few lodgepole pine, and occasional spruce saplings. The mineral soil in the unburned spruce stand is overlain by an organic layer up to 10 cm thick.

The valley is in the sporadic permafrost zone (Heginbottom 1995), and less than 20% of the test holes drilled in the valley in connection with the Alaska Highway gas pipeline proposal encountered frozen ground (Rampton et al. 1983). Geotechnical drilling in 1978 at two sites in the burned area encountered ice-rich permafrost from 3 m below the ground surface to depths of 9.5 m, where drilling ceased (Klassen 1979). Drilling at four other sites in the burned area in 1982 (Fig. 2*b*) indicated that ice-rich permafrost lay 4.0–4.5 m below the ground surface (Burn 1987). Two of these sites were drilled in a moist area adjacent to the valley side, where there had been some regeneration of mosses and thick ground cover since the fire. At these sites, the appearance of ice grains in the drill core between 2 and 2.8 m suggested permafrost degradation had been arrested.

Fig. 5. (*a*) Gravimetric water content of drill core retrieved from the forest (□) and burned (▲) sites in July 1990. (*b*) Excess ice content of the same cores. In the uppermost 150 cm, the soil at the forest site is generally coarser than that at the burned site, and, hence, is drier. Note that an excess ice content of 0% does not imply that the ground is saturated.

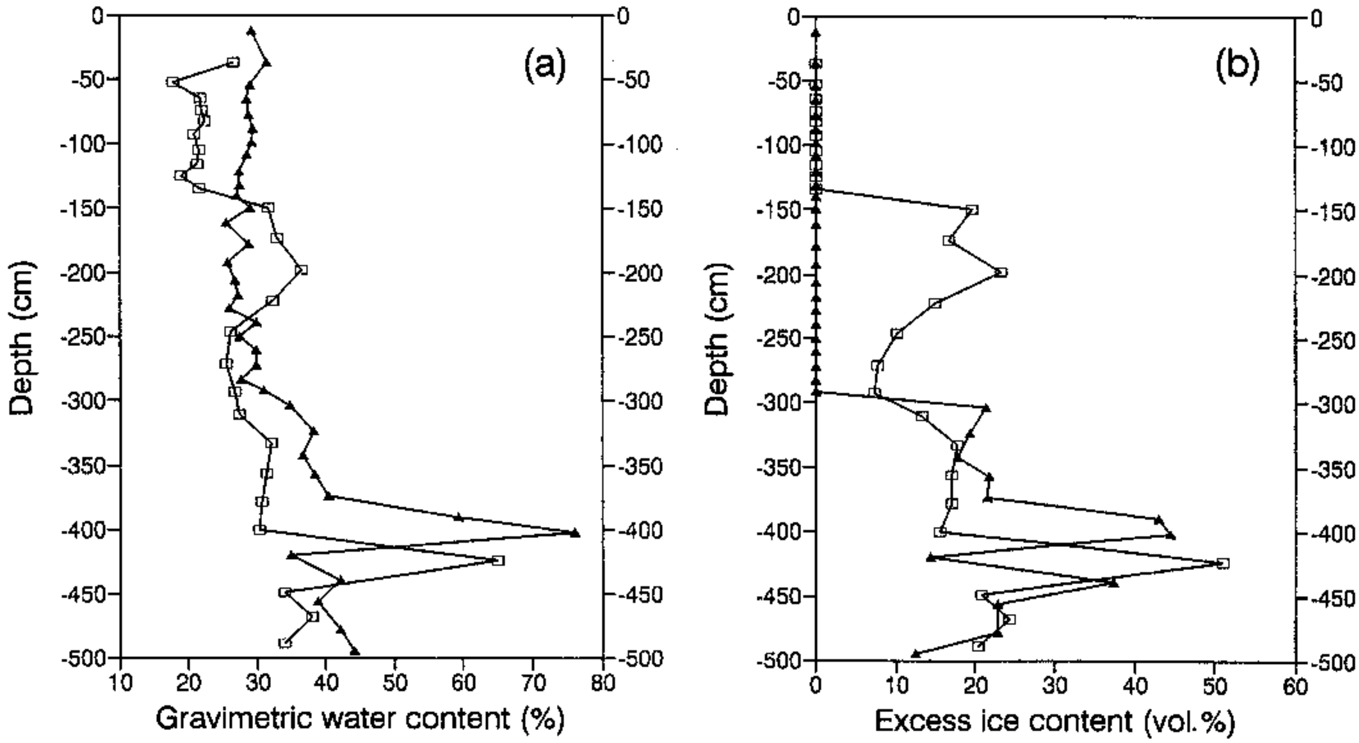

Methods

Fieldwork began in summer 1982, with drilling to 5 m depth at several sites to establish the cryostratigraphy and to install thermistor cables for ground temperature monitoring. These temperatures were measured sporadically for 2 years at sites in the forest and the burned area, including an open meadow. Subsequently, most measurements between 1984 and 1990 were made in winter. At these sites, thermistors were located at 0.5, 1.0, 1.5, 3.0, and 5.0 m depths. Data collection continued through to 1996 at the forest and meadow sites, although many of these thermistors have now failed. These sites offer contrasting thermal regimes, as the ground beneath the forest is perennially frozen, whereas there is no permafrost at the meadow site.

In July 1990 further drilling was completed in the forest and burned area. At both sites, permafrost was penetrated by water-jet drill, a 1-in. steel pipe was lowered to case the hole, and thermistor cables were installed to measure the temperature profile throughout permafrost (Fig. 3). The cable installed in the forest remains operational, but the installation in the burned area was vandalized in June 1991 and a new cable was installed in August 1995. Ground temperatures were originally measured on sensors fixed at vertical intervals of 3 m throughout the cased hole, but only a single bead was used in 1995, and measurements have been made at intervals of 1 m at this site by hauling the cable up the casing. Near-surface thermistors were also installed at forest and burned sites in July 1990, at depths of 0.5, 1.0, 1.5, 2.0, 3.0, 4.0, and 5.0 m, in holes drilled with a core barrel. The water content of the drill core from these holes was determined shortly after recovery. All thermistors were calibrated in an ice bath during cable construction, and ground temperatures are reported here to the nearest 0.1°C. Ground temperature measurements from the holes took 3–6 months to stabilize and only data collected from 1991 onwards are reported.

In 1994, two HOBO miniature air temperature loggers, manufactured by Onsett Corporation, were installed in the burned and forest areas, to compare air temperatures between the two sites and with respect to the regional weather station at Whitehorse Airport. The loggers were placed in radiation shields, which allow the free passage of air around the sensors (Fig. 4). The loggers measure air temperature five times daily, and the record has been interrupted only once, during a cold spell in January 1996. The loggers have a factory-specified precision of ±0.13°C and a range of −37.3°C to 46.0°C. The lower limit has been exceeded during some frigid periods, but the upper limit has not. Laboratory calibration of several similar loggers has confirmed the manufacturer's precision specifications.

The data presented below emphasize near-surface ground temperature measurements made at least every 6 weeks, and usually more frequently, between August 1990 and December 1996, at forest, burned, and meadow sites. The absence of summer data limits the utility of measurements collected between 1984 and 1990. The burned site was drilled again in August 1997 to confirm the location of the permafrost table.

Near-surface earth materials

Jet drilling at the burned site indicated that the uppermost

Fig. 6. Unfrozen water content (θ_u) characteristic curve for remoulded silty clay from the burned site, determined by time domain reflectometry (Patterson and Smith 1981). Each point represents the mean unfrozen water content of five samples at the respective temperature. The absolute error in volumetric unfrozen water content is ±2.5%. The curve was derived during incremental warming of the soil samples from –4°C. Equation [1], $\theta_u = 14.41T^{-0.39}$, where T is temperature (°C) below 0°C, is displayed as the fitted line.

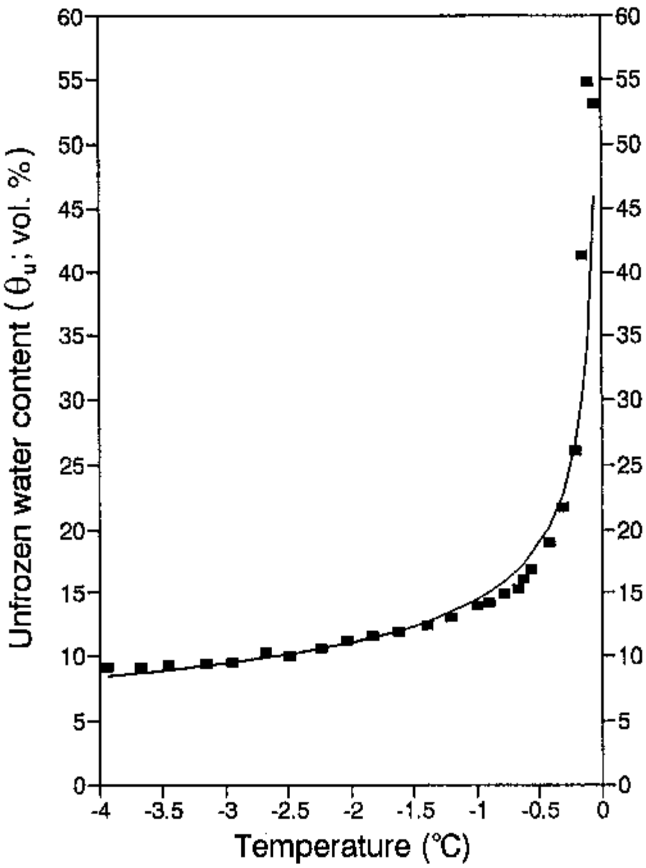

9–12 m comprises fine-grained sediments, as reported by Klassen (1979). Nine drill-core samples collected at 50 cm intervals in the uppermost 5 m at the site contained no sand (>63 μm), and sediment was evenly split between the silt- and clay-size fractions at 4 μm; 40% of the material was <2 μm. Below 9 m, well-bonded, frozen sandy beds, up to 50 cm thick, were encountered. Sand dominates the sediment texture beneath the base of ice-bonded permafrost, which was at 16 m in 1990.

At the forest site, the ground is covered by 15 cm of mosses, lichens, and other organic matter. The uppermost 6 m of mineral material is composed of fine sands and finer grained sediments. Particle-size analyses of drill core indicated 71% of sample material in the sand fraction, 14% silt, and 15% clay. A lens of sediment of similar composition to the sediments at the burned site was recorded between 0.5 and 1.5 m depth. Below 12 m, the material is dominated by coarser sands. The base of ice-bonded permafrost is at 16.5 m.

Figure 5*a* presents the gravimetric water (ice) content of drill core collected continuously in the same holes, indicating that, characteristically, the moisture content of permafrost is higher than that in the active layer (Cheng 1983; Mackay 1983). The excess ice content, presented in Fig. 5*b*, is the volumetric proportion of ice in the soil over and above the ice content at saturation, when all the pore space is occupied. The saturation ice content was determined from the water content of core samples from recently thawed soil collected immediately above ice-rich permafrost. Excess ice content is a measure of minimum settlement that may occur upon thawing, without regard for soil consolidation. In the uppermost permafrost of the burned area, the average excess ice content of permafrost is 24%, indicating that for each metre of ground thawed, at least 24 cm of subsidence may occur. Several of the thermokarst lakes in the study area have burned trees standing in them, demonstrating postfire subsidence.

The unfrozen water content characteristic for the glaciolacustrine sediment, determined by time domain reflectometry, is presented in Fig. 6. During ground warming, the gradient of the relation visibly increases with temperature above –0.5°C, indicating the temperature range in which ground warming may stall, as latent heat effects increase (Riseborough 1990). The relation between unfrozen water content (θ_u, vol.%) and temperature below 0°C (T, °C), determined from the functional fit of a logarithmic transformation of Fig. 6 (Mark and Church 1977), is

$$[1] \quad \theta_u = 14.41T^{-0.39}$$

Air and near-surface ground temperatures

Air temperature regime

Figure 7 is a scatter plot of daily mean air temperatures recorded at burned (T_B) and forested (T_F) sites from 21 July 1994 to 29 June 1996. The relation derived from a functional fit to the variables, here the principal axis because the precision of the observations are identical (Mark and Church 1977), is

$$[2] \quad T_B = 0.99T_F + 1.25 \qquad n = 665;\ r^2 = 0.99$$

These data indicate that air temperatures in the burned area (T_B) are consistently warmer than in the forest (T_F), by about 1.25°C (see Zhou et al. 1993). The difference demonstrates that shade effects a consistent influence on temperature throughout the year. The functional relation between daily mean air temperature at Whitehorse Airport (T_W) and the burned site is

$$[3] \quad T_B = 1.08T_W - 1.07 \qquad n = 688;\ r^2 = 0.97$$

Takhini valley is slightly cooler than Whitehorse Airport, the long-term weather station for south-central Yukon Territory.

Near-surface ground temperatures

Daily mean ground temperatures at 20 cm depth for the burned and forested sites are displayed for 1994–1995 in Fig. 8. The summary principal axes for the summer and winter periods are distinct, with ground temperatures consistently warmer at the burned site, although the snow cover at the two sites is comparable in depth and density (Fig. 9). Heat released from storage in the deeper active layer retards near-surface cooling at the burned site. Two relations, defined by the principal axes, describe the influence of burning on near-surface ground temperatures (Fig. 8). In summer, when ground temperatures are

Fig. 7. Scatter plot of air temperatures measured at the forest (T_F) and burned (T_B) sites, 21 July 1994 to 29 June 1996.

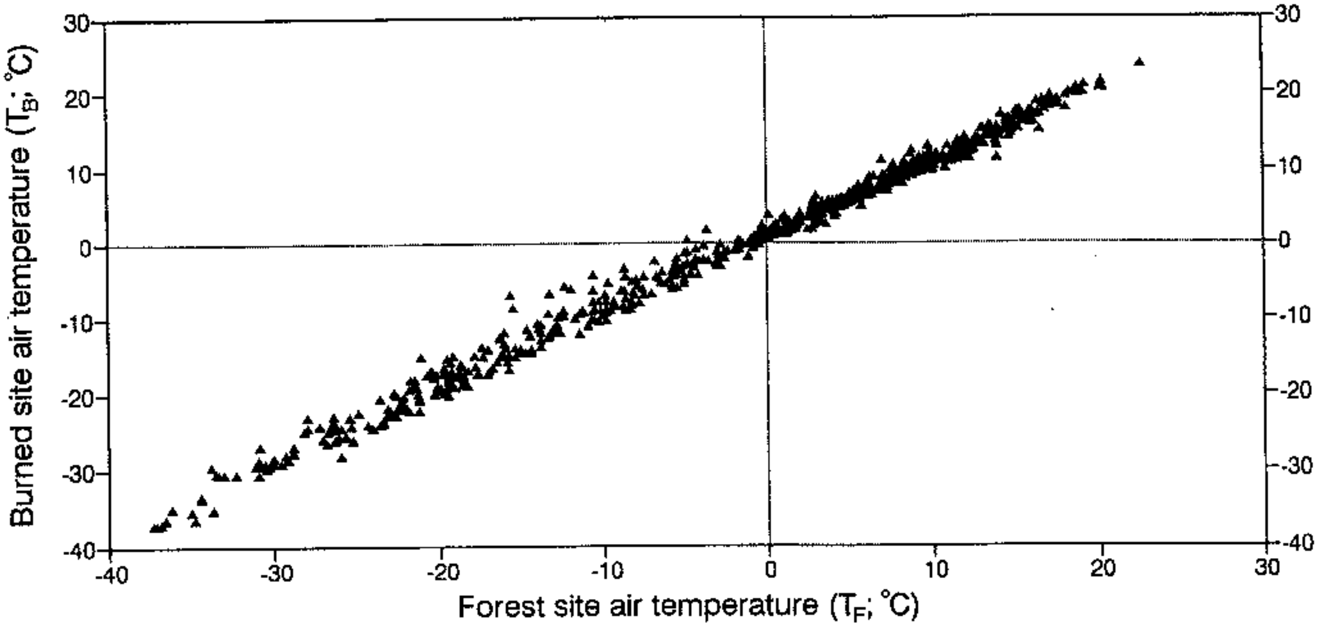

Fig. 8. Scatter plot of daily mean ground temperatures at 20 cm depth measured at the forest (T_{F20}) and burned (T_{B20}) sites, 21 July 1994 to 9 June 1995, when the cable at the burned site was chewed. Separate relations are derived for the summer and winter periods. For the summer, $T_{B20} = 1.24T_{F20} + 1.44$ ($n = 127$; $r^2 = 0.97$); in winter, $T_{B20} = 0.55T_{F20} - 0.11$ ($n = 199$; $r^2 = 0.94$).

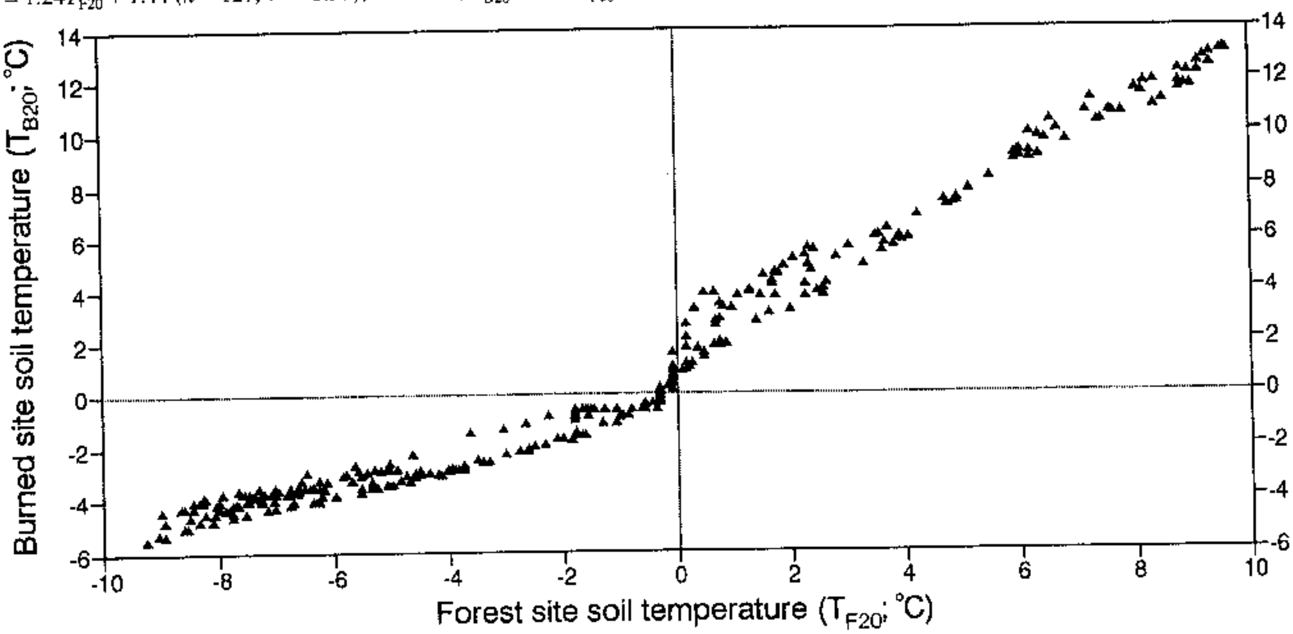

above 0°C, the burned site is 1.5°C or more warmer than the forest site at 20 cm depth. As the temperature declines in winter, the difference between the sites increases, with the burned site warmer. Soil temperatures collected at 50 cm depth, between 1991 and 1996, demonstrate seasonal relations similar to those displayed in Fig. 8. However, the scatter increases with the depth of the points of measurement, because of variations in the thermal properties of the overlying materials. There is relatively small variation in 50 cm winter ground temperatures at the burned site in comparison with undisturbed conditions.

The *n*-factor

The *n*-factor, the ratio of air to ground thawing or freezing degree-days, is used in engineering to summarize the relation between air and ground temperatures (Lunardini 1978). Generally, *n*-factors have been determined for artificial surfaces, but they have been derived for natural surfaces to assist in modelling regional permafrost conditions (Lunardini 1978; Jorgenson and Kreig 1988; Taylor 1995). The *n*-factors derived for natural surfaces are site specific, partly because of the spatial variability of snow cover.

Figure 10 indicates air and 20 cm ground temperatures at

Fig. 9. Plot of active-layer development and snow cover at forest (□) and burned (▲) sites over an illustrative year, 1 April 1993 – 30 April 1994. The extent of the active layer is defined from the location of the 0°C isotherm(s), interpolated from ground temperature measurements. The snow density, determined on the days of depth observations, was almost the same at each site, ranging over the winter between 0.15 and 0.20 g·cm^{-3}.

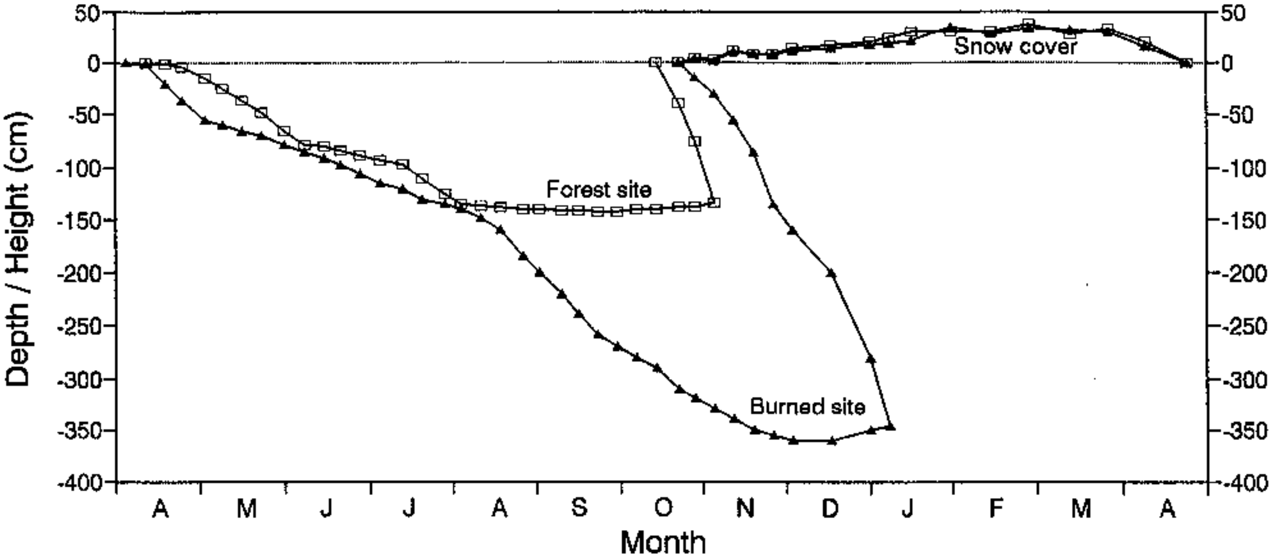

Fig. 10. Scatter plot of air and 20 cm ground temperatures measured at the burned site, 21 July 1994 to 9 June 1995; see eqs. [4] for summary relations. ■, summer; □, winter; ▲, spring.

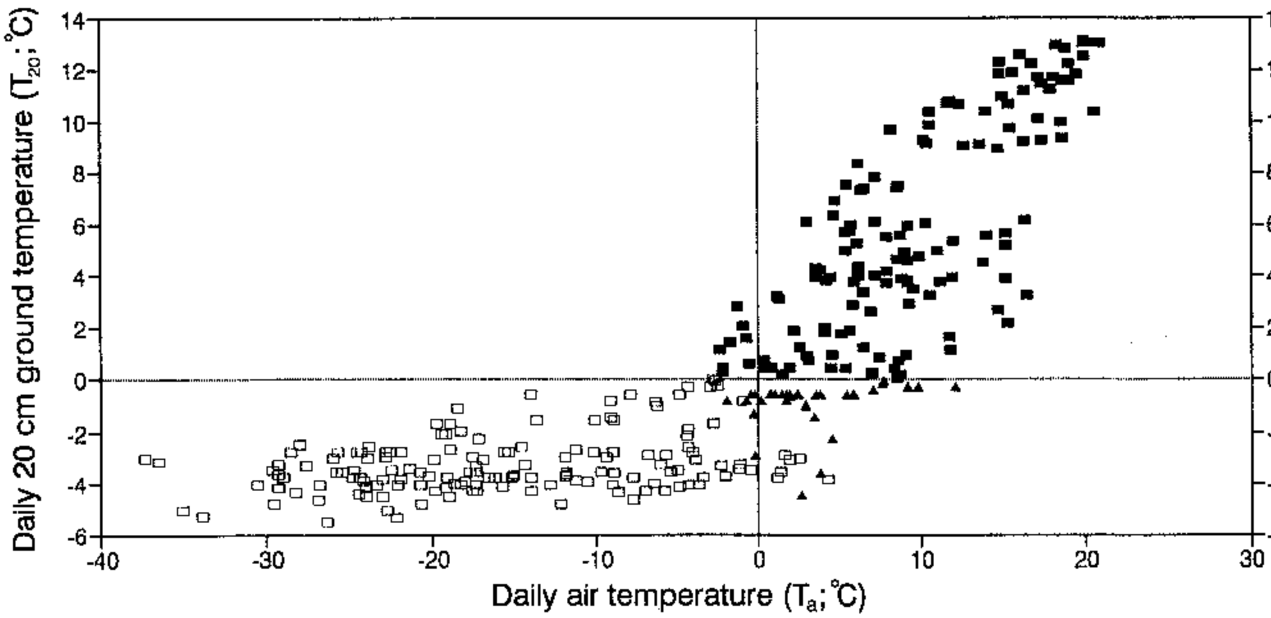

the burned site from 21 July 1994 to 9 June 1995. These data are scattered, but may conveniently be divided into three seasons: (*a*) winter, from mid-October to the end of March, when both air and ground temperatures are below 0°C; (*b*) spring, in April, when snowmelt occurs, and daily mean air temperatures rise above 0°C; and (*c*) summer, from May to mid-October, when both air and 20 cm ground temperatures are above 0°C. Equations [4], the principal axes derived for each season, summarize the relations between air temperature (T_a) and 20 cm ground temperature (T_{20}) for the respective periods at the burned site:

[4*a*] $T_{20} = 0.03T_a - 2.94$ $n = 147$; $r^2 = 0.07$ (winter)

[4*b*] $T_{20} = 0.07T_a - 1.16$ $n = 34$; $r^2 = 0.05$ (spring)

[4*c*] $T_{20} = 0.57T_a + 0.45$ $n = 143$; $r^2 = 0.63$ (summer)

Table 2. Summer and winter n-factors for the burned and forested sites, determined by freezing and thawing indices, and by the slope of the relation between air and soil temperatures measured at the sites, and air temperature at Whitehorse Airport.

Burned site 22 July 1994 – 09 June 1995

	TDD (deg-day)	FDD (deg-day)	n-factor by index		n-factor by line	
			n_t	n_f	n_t	n_f
Air temperature	1429	2398	0.55	0.22	0.57	0.07
Soil temperature	783	530				
Whitehorse Airport	1490	2030	0.53	0.26	0.60	0.07

Forest site[a]

	TDD (deg-day) 1995	FDD (deg-day) 1994–1995	FDD (deg-day) 1995–1996	n-factor by index n_t 1995	n_f 1994–1995	n_f 1995–1996	n-factor by line n_t 1995	n_f 1994–1995	n_f 1995–1996
Air temperature	1763	2639	(2197)[b]	0.50	0.35	(0.24)[b]	0.61	0.25	(0.26)[b]
Soil temperature	878	927	761 (522)[b]						
Whitehorse Airport	2000	2027	2520	0.44	0.46	0.30	0.66	0.28	0.25

Notes: TDD, thawing index; FDD, freezing index

[a] Data are compiled for complete seasons.

[b] The air temperature logger failed in January 1996, after exposure to conditions below –40°C, and was replaced 3 weeks later. The results in parentheses refer to the portion of winter for which data are available.

Fig. 11. Six-year time series, beginning in January 1991, of 1.5 m ground temperatures at forested (□) and burned (▲) sites, Takhini River valley. The 6-year mean temperatures at this depth are –0.8°C and 0.1°C for the forest and burned sites, respectively.

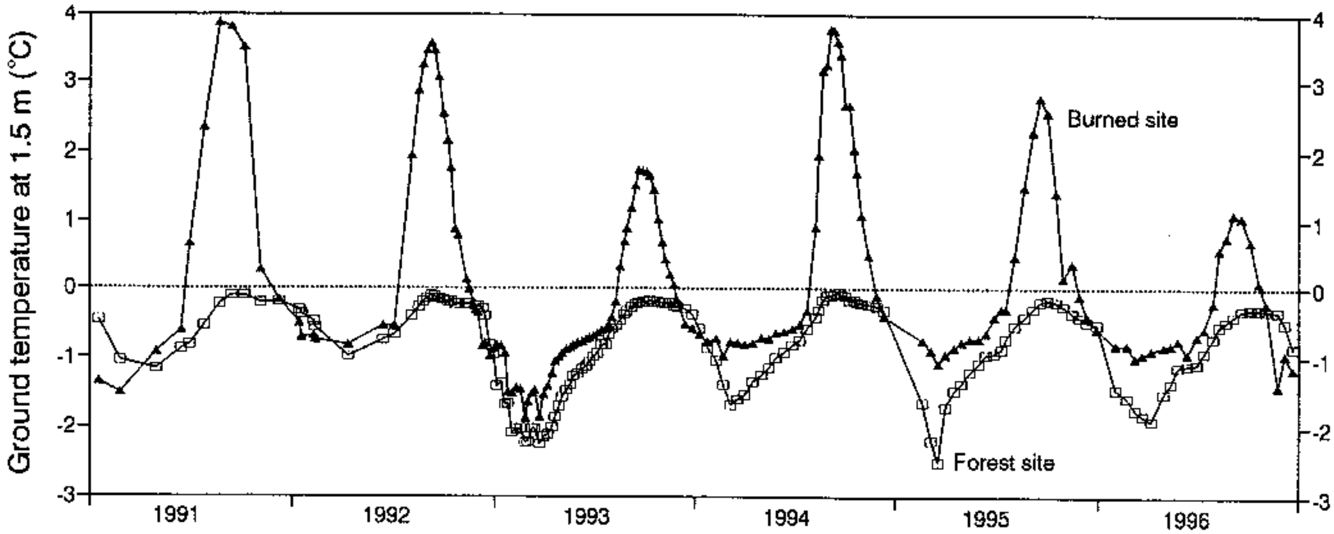

The relation between air and ground temperature is clearest in summer, that is, the coefficient of determination (r^2) is greatest, when there is no snow. The respective relations for ground temperature at the burned site with respect to air temperature at Whitehorse Airport are

[5a] $T_{20} = 0.03T_a - 2.95$ $\quad n = 147;\ r^2 = 0.07$ (winter)

[5b] $T_{20} = 0.09T_a - 1.24$ $\quad n = 34;\ r^2 = 0.08$ (spring)

[5c] $T_{20} = 0.60T_a - 0.19$ $\quad n = 143;\ r^2 = 0.69$ (summer)

The n-factors are usually calculated from the sums of freezing or thawing degree-days, but when the intercept approaches zero, the n-factor is equivalent to the slope of the relations presented in [4] and [5]. The n-factors calculated by both methods are presented in Table 2, demonstrating a consistency in estimate of thaw-season n-factor (n_t). Equations [4] and [5] indicate that, with low r^2, the relation between winter air and 20 cm soil temperature is poorly defined at the burned site. The near-surface ground temperature may be summarized best as constant over the winter and spring periods at the level of the respective intercepts. At the burned site, the n-factor method is of most utility in summer.

At the forest site, n_t is lower than for the burned site, but the freezing-season n-factor (n_f) is higher, indicating that the ground is cooler beneath the forest throughout the year. The n-factors derived from the principal axes are noticeably different from those calculated by ratio both in summer and winter,

Fig. 12. Time series of daily mean ground temperatures at 20 cm depth at forested (□) and burned (▲) sites, Takhini River valley, 21 July 1994 to 9 June 1995.

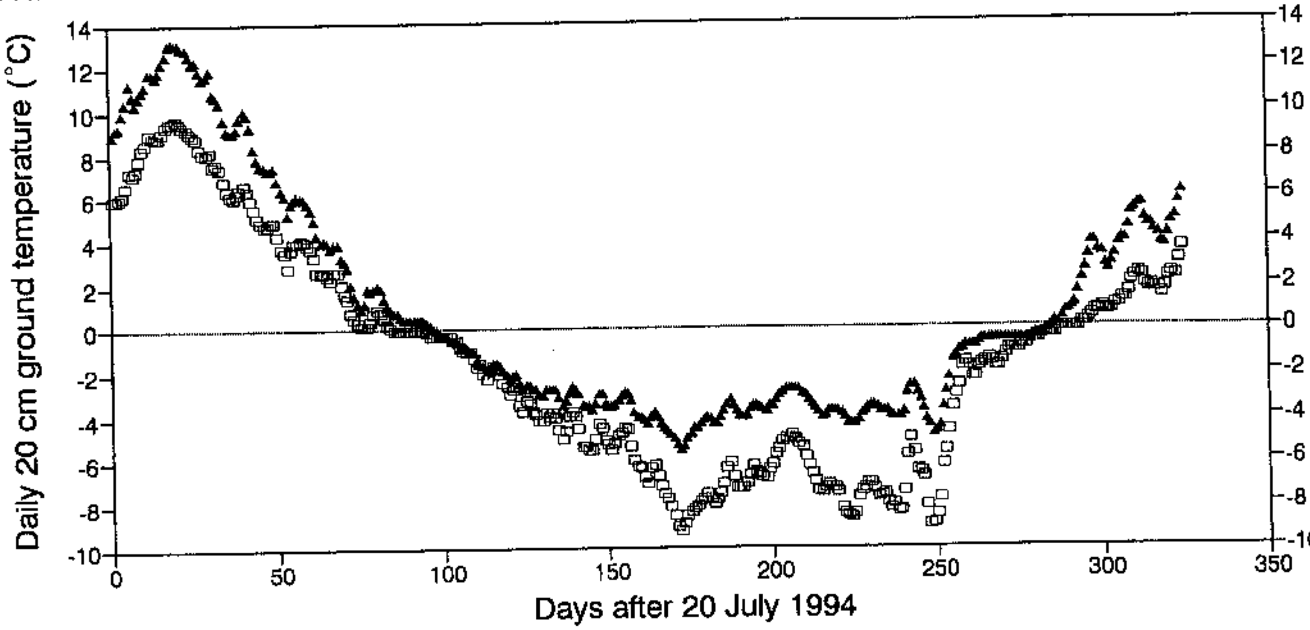

in association with low values for r^2. The functional relations for air and 20 cm ground temperatures at the forest site in winter, spring, and summer are, respectively,

[6a] $T_{20} = 0.29T_a + 0.39$ $n = 327$; $r^2 = 0.35$ (winter)

[6b] $T_{20} = 0.46T_a - 2.04$ $n = 91$; $r^2 = 0.21$ (spring)

[6c] $T_{20} = 0.55T_a - 0.37$ $n = 253$; $r^2 = 0.36$ (summer)

These relations and the data in Table 2 are comparable to the mean determinations by Taylor (1995) of 0.59 and 0.20 for n_t and n_f from several natural sites in Mackenzie River valley, N.W.T. The single values for the n-factors, however, mask considerable variation in the relations at subseasonal time scales.

The n-factors determined by both methods are comparable at the two sites in summer, when the ground heat flux is downwards. In winter, the n-factors are considerably different, even though snow conditions and air temperatures are similar. During winter, the ground heat flux is upwards and originates from a warmer body at the burned site. These data indicate the importance of subsurface conditions on near-surface temperatures in winter, and, hence, the n-factor.

Ground thermal regime

Temperatures at the top of permafrost

Figure 11 displays time series of ground temperature at 1.5 m for forested and burned sites. The sensor at the forest site is in permafrost, but in the burned area it is in the active layer. The data show maximum divergence of these series in summer. In contrast, Fig. 12, prepared from data collected in 1994–1995 only, suggests a more consistent difference at 20 cm, with ground temperatures warmer at the burned site throughout

Fig. 13. Mean annual ground temperature profiles throughout permafrost, for forested (□) and burned (▲) sites, compiled from observations made over 6 years beginning in January 1991.

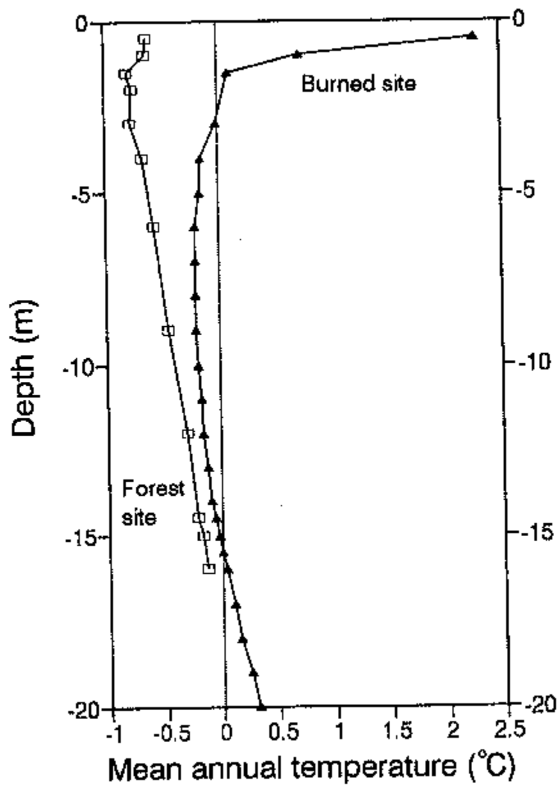

most of the summer and winter. The temperature series in Fig. 12 converge during fall freeze up and snow melt, when differences in surface conditions are subsumed by the effects of latent heat. The distinct differences at 1.5 m depth in

Fig. 14. Ground temperature profiles for the burned site measured on 14 June 1991 (■) and 29 June 1996 (☒). In 1991 instrumentation at the site comprised a set of cables with sensors at fixed depth intervals; the site was vandalized a few days after this recording. Subsequently a single cable has been installed, and this is hauled up the access pipe to provide measurements at various depths.

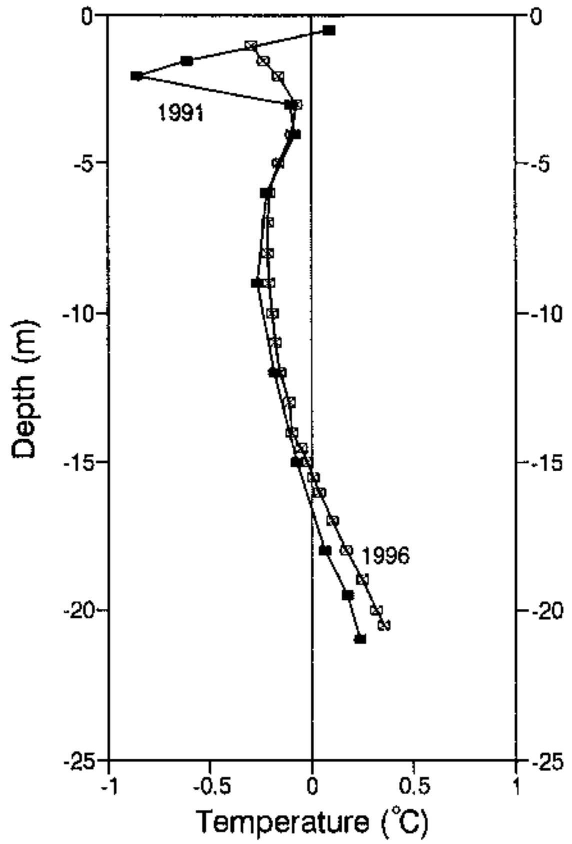

summer (Fig. 11) are due to ground ice at the top of permafrost, which restricts the maximum ground temperature to <0°C at the forest site (see Fig. 6). The burned site is warmer in winter, due to heat released from storage lower in the profile. Overall, the mean temperature at the level equivalent to the top of permafrost at the burned site has been raised above 0°C. While the change in surface conditions has led to a difference in air temperature of 1.25°C between the sites, the ground temperature at the level of the top of permafrost has risen by 0.9°C.

Temperature profile through permafrost

The base of permafrost at the burned site is at 15.5 m depth, but the base of ice-bonded permafrost at the forest site, determined by jet drilling, was at 16.5 m in 1990, and the base of permafrost per se, estimated by linear extrapolation from the temperature profile, is at 18.5 m (Fig. 13). The linear increase of ground temperature with depth below the active layer at the forest site, $0.05°C \cdot m^{-1}$, indicates that permafrost at this site is in equilibrium with surface conditions. Similar ground temperature gradients have been reported from other sites in southern Yukon (Burgess et al. 1982). There is a thermal offset of 0.2°C in the active layer between 0.5 and 1.5 m, but it is small

Fig. 15. Minimum ground temperature profiles above permafrost at the burned site, recorded in 1992 (■) and 1993 (☒). These data represent, respectively, the warmest and coolest minimum temperature profiles measured at the site between1991 and 1996.

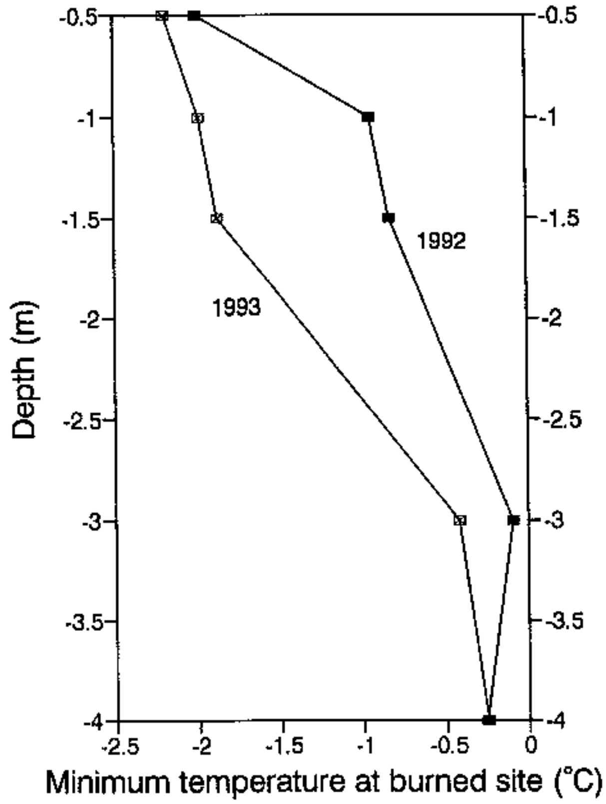

because the site is dry (see Fig. 5*a*), minimizing the seasonal variation in thermal properties of surficial materials (Burn and Smith 1988).

Mean annual ground temperatures at the burned site of −0.2°C or higher at all depths indicate warming throughout the profile with respect to undisturbed conditions (Fig. 13). The mean annual temperature between 1991 and 1996 at 3 m was 0°C, but the top of permafrost was lowered from 3.50 to 3.75 m depth between July 1990 and August 1995. The apparent thermal offset at the site is over 2°C, but this represents the continuing transition in the ground thermal regime between permafrost and non-permafrost states, rather than an equilibrium condition.

The temperature profile at the burned site (Fig. 13) indicates that heat is being supplied to warm permafrost from above and below the frozen ground. Artesian water flow at the burned site, observed for a day after drilling, indicates that the temperature below permafrost may be sustained, in part, by groundwater convection in the underlying sands. The aquifer at the site is unlikely to be totally confined, because of the discontinuous distribution of permafrost in Takhini Valley. Figure 14 indicates ground temperature profiles from 1991 and 1996 at the burned site, illustrating a slight warming of permafrost (by <0.1°C) throughout the profile over the period, which has involved melting a considerable quantity of pore ice ($0.05\ cm^3 \cdot cm^{-3}$; see Fig. 6). During the same period, the base of permafrost has risen by about a metre, and the top of permafrost has been lowered by 25 cm. If the field data are

Fig. 16. Ground temperatures at the forest (□) and meadow (■) sites, 1983–1996. The mean temperature at the meadow site is 2°C, measured at 5 m depth. At the forest site the mean temperature is –0.75°C, from 3 m depth. There are no clear temporal trends in the data sets.

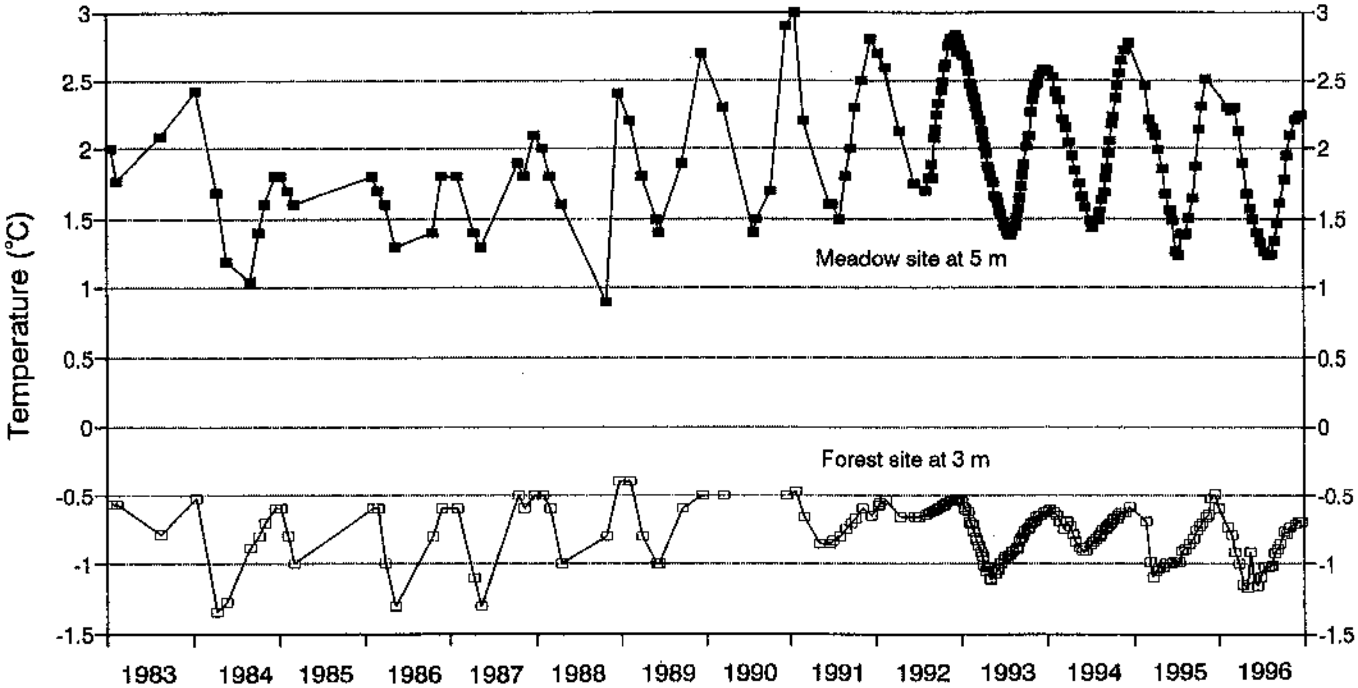

correct, they indicate the addition of convective heat to the base of permafrost, because conduction alone would be insufficient to thaw this amount of ground. Convection may be facilitated in the sandy sediments below permafrost.

Active-layer development

Harris et al. (1988, p. 13) define the active layer as "the top layer of ground subject to annual thawing and freezing in areas underlain by permafrost." As Mackay (1995, p. 325) has pointed out, this definition is often impossible to use in the field, and here we adopt the traditional definition for the base of the active layer at the 0°C isotherm (Muller 1947).

Thawing of the active layer begins in April at the burned site, but several weeks later in the forest, due to the persistence of the snow pack in the shade (see Fig. 9). At the forest site, the active layer is 1.40–1.45 m deep, and thaws to its maximum depth in mid-September. At the burned site, thaw penetration is deepest in October or November, and is increasing annually. In 1996, the thickness was estimated at 3.80 m. Freeze-back of the active layer is not complete at the burned site until January, although frost penetration begins in October.

Minimum temperatures recorded in the active layer at the burned site are summarized in Fig. 15, which indicates that the active layer froze back, that is, the temperature fell below 0°C, each autumn between 1990 and 1996; at 3 m depth, the ground usually cooled to –0.3°C. Comparison of Figs. 5*a* and 6 indicates that about one third of the pore water in the moist soil above permafrost freezes during cooling to this temperature. A layer of thawed ground between the base of the active layer and degrading permafrost, or a "residual thaw layer" (Harris et al. 1988, p. 74), has not been observed at this site. Murton and French (1993) suggest that a paleothaw layer was widespread in permafrost terrain of the Tuktoyaktuk coastlands during the early Holocene warm interval, although the depth of thaw above permafrost was generally less than 1.7 m (Murton et al. 1995; Burn 1997). The data from Takhini demonstrate that an active layer twice as thick may freeze back even above thawing permafrost and with a relatively warm winter ground surface temperature regime. A residual thaw layer may occur at the burned site in the future when the permafrost table is several metres farther below the surface.

Degradation of permafrost following forest fire

Ground temperature trends, 1983–1996

Figure 16 presents ground temperature series obtained at the forest and meadow sites from 1983 to 1996. The forest site is underlain by permafrost, but the meadow site is in unfrozen ground. While the data presented are from different depths, neither is within the active layer. Figure 16 demonstrates the distinct thermal regimes of the two sites, with overall mean ground temperatures differing by 2.75°C. The amplitude of the annual fluctuation is greater at the meadow site, where there is minimal latent heat exchange in the dry soil. There is no overall temporal trend at either site, suggesting that ground temperatures have been stable at sites where permafrost is not degrading. Ground temperatures at the burned site, where permafrost is degrading (see Figs. 11 and 13), are transitional between these two states. The mean annual temperature at the burned site is now 2°C at 0.5 m depth, demonstrating evolution of the thermal regime at this site from that characteristic of a site with permafrost to one without it. The change in surface conditions effected by the fire presently dominates the spatial and temporal variation in ground temperatures of Takhini River valley.

Fig. 17. Running mean of the preceding 12 months' air temperature at Whitehorse Airport, 1959–1996, plotted from monthly means supplied by Environment Canada.

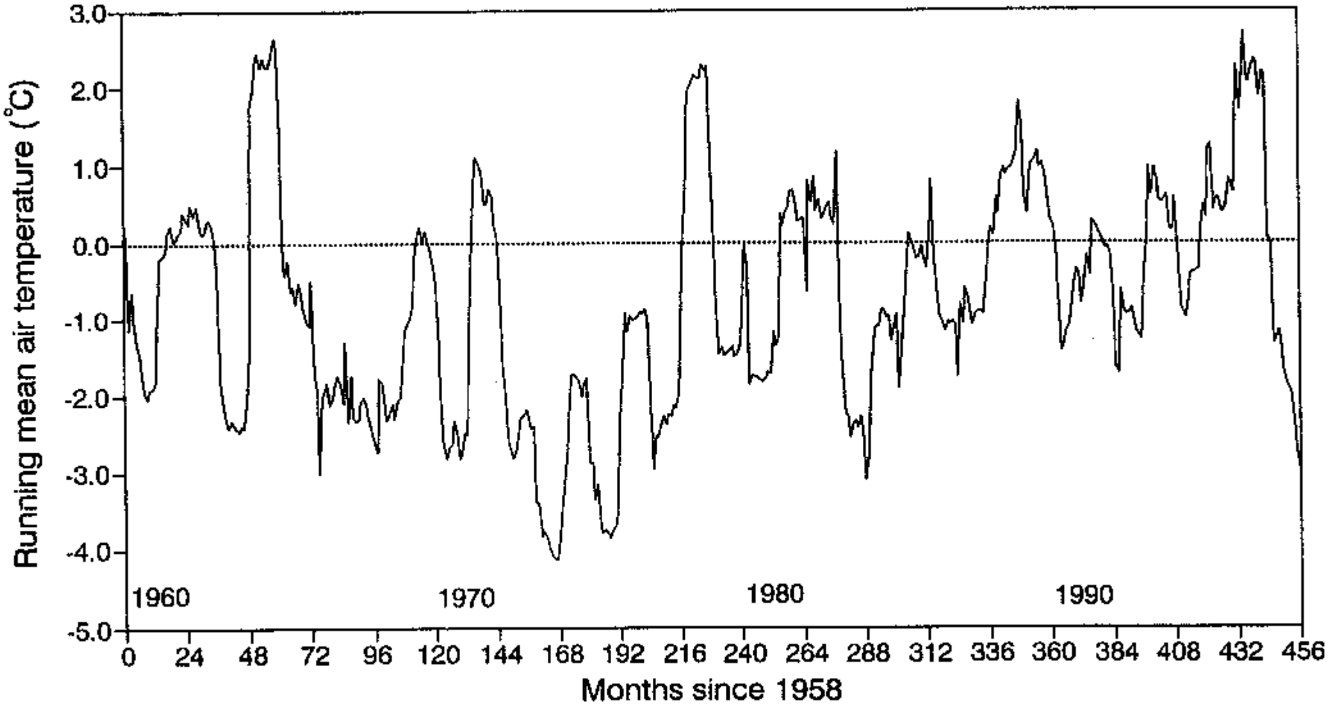

Climate trends

Figure 17 indicates mean air temperatures recorded at Whitehorse Airport since the Takhini Valley fire. The data are presented as the running mean of the preceding 12 months' observations (1959–1996). The overall mean of this index is –0.78°C, with standard deviation 1.48°C ($n = 467$). There is a discernible decrease in mean temperature at a rate of –0.1°C·a^{-1} from 1960 to the early 1970s, with a minimum running mean of –4.0°C determined in 1971–1972. Subsequently, air temperatures have risen at an overall rate of 0.1°C·a^{-1} to a maximum running mean of 2.7°C in 1994–1995. The raw data suggest that these trends are a function of winter conditions, as demonstrated by Burn (1992) for central Yukon, because there is more variation in winter than summer temperatures. The effect of variability in winter temperatures on the ground thermal regime is attenuated by snow cover, as demonstrated in Fig. 8. The significance of climatic variation since the fire for ground temperatures has clearly been considerably less than the effects of the change in surface conditions, because ground temperatures at the forest and meadow have remained relatively stable during 14 years of slight climatic warming (Fig. 16). In the following analysis of permafrost degradation, the climate is considered effectively constant over the period of interest.

Permafrost degradation

The depth to the top of permafrost at the burned site has been determined by drilling four times since the fire: 3 m in 1978 (Klassen 1979); 3.50 m in 1990; 3.75 m in 1995; and 3.80 m in 1997. In the following analysis, we assume that active-layer thickness before the fire was 1.40 m at the burned site. Figure 18 indicates the relation between the increase in active-layer thickness, or permafrost degradation, and time since 1958. The data plot as a straight line when time is transformed by its square root. The intercept of the line approximates the origin, and the slope of the line is 0.38. The line indicates that 1.2 m of permafrost degradation likely occurred in the decade following the fire.

The Stefan solution for freezing or thawing of frozen ground has been used to describe active-layer development (e.g., Mackay 1995), and the thaw of permafrost beneath thermokarst lakes (Burn and Smith 1990). The solution prescribes thaw penetration into homogeneous frozen ground, initially isothermal at 0°C, following a step rise in surface temperature to an invariant value. The solution relates z, the depth of thaw (m), to k, the thawed soil thermal conductivity (J·a^{-1}·m^{-1}·°C^{-1}), L, the latent heat of fusion (J·m^{-3}), T_s, the surface temperature (°C), and t, the time since thawing began (a) (e.g., Andersland and Ladanyi 1994, p. 73):

$$[7] \quad z = (2kT_s t/L)^{1/2}$$

Equation [7] is often rewritten:

$$[8] \quad z = bt^{1/2}$$

where

$$[9] \quad b = (2kT_s/L)^{1/2}$$

The data in Fig. 18 are summarized by the line

$$[10] \quad z = 0.38t^{1/2} + 0.03$$

The intercept is near the origin, and b of [8] is 0.38 m·a$^{-1/2}$.

Interannual variations in b are to be expected due to changes in annual climate, soil moisture, and ice content of thawing permafrost. Romanovsky and Osterkamp (1997) point out that cold temperatures below the thawing zone may invalidate application of the Stefan solution to estimating active-layer

Fig. 18. Increase in depth of active layer, i.e., permafrost degradation, at the burned site since 1958. Time has been transformed to its square root to illustrate the Stefan behaviour of the data set; the datum for 1978 is from a site adjacent to the location of the temperature cable in the burned area (Klassen 1979; see Fig. 2*b*). The slope of the fitted line is 0.38, the intercept is 0.03, *n* is 5, and r^2 is 0.99.

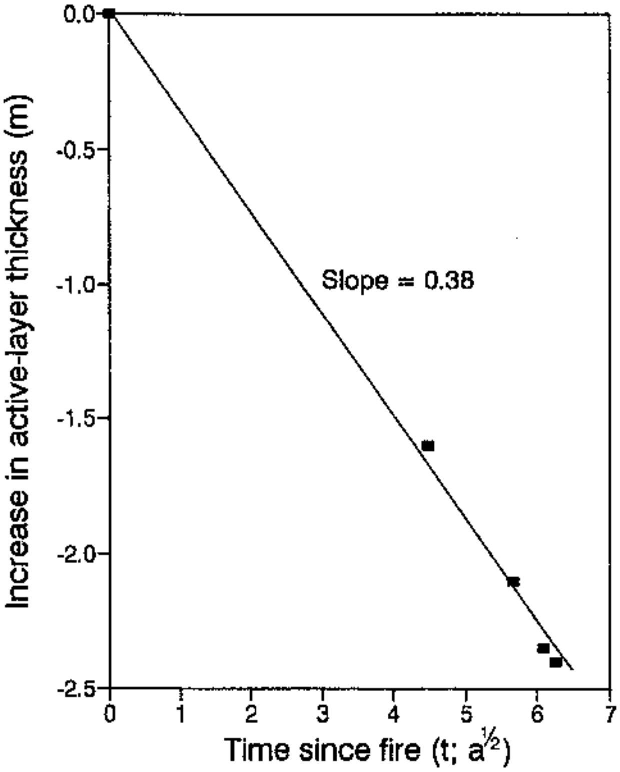

Table 3. Calculation and sensitivity analysis of Stefan's *b* from thermal properties of soils at the burned site.

n^a (%)	Ei^b (%)	k^c (10^7 J·a^{-1}·m^{-1}·°C^{-1})	L^d (10^8 J·m^{-3})	T (°C)	b^e (m·a$^{-1/2}$)
50	24	3.86	1.88	0.1	0.20
50	24	3.86	1.88	0.2	0.29
50	24	3.86	1.88	0.3	0.35
50	24	3.86	1.88	0.4	0.41
50	0	3.86	1.51	0.2	0.31
50	0	3.86	1.51	0.4	0.45
40	0	4.61	1.21	0.2	0.39
40	0	4.61	1.21	0.4	0.55
50	48	3.86	2.24	0.2	0.26
50	48	3.86	2.24	0.4	0.37
40	48	4.61	2.08	0.2	0.30
40	48	4.61	2.08	0.4	0.42

[a]Porosity, estimated from mass of water in saturated samples retrieved immediately above permafrost.

[b]Excess ice content, estimated from $(V_W - m_s n/\rho)/V_T$ for core samples retrieved from permafrost, where V_W is total water content of core sample, V_T is volume of sample, m_s is mass of sample, and ρ is bulk density.

[c]Thermal conductivity of thawed soil (Johansen 1975): $k_s^{(1-n)} k_w^{n}$, where k_s is thermal conductivity of mineral material (3.0 W·m^{-1}·°C^{-1}), k_w is thermal conductivity of water (0.5 W·m^{-1}·°C^{-1}).

[d]Latent heat of fusion: $3.03 \times 10^8 \times V_W$ (J·m^{-3}).

[e]$b = (2kT/L)^{1/2}$ (m·a$^{-1/2}$).

development (see also Burn 1997). Here, the model is not applied to active-layer development, that is, seasonal thawing, but to long-term permafrost degradation. Furthermore, the Stefan model accounts for only conductive heat transfer. Hinkel et al. (1997) have demonstrated convection within the active layer, due to infiltration of precipitation, and internal distillation during freeze-back, but the extent to which convective effects modify the conductive regime is not clear. It is, therefore, instructive to compare the apparent efficacy of the Stefan model as calibrated from a record of thawing (Fig. 18) with an estimate derived from ground thermal properties and temperatures.

The volumetric ice content of the permafrost at both sites is about 62%, while the volumetric water content above permafrost in the silty clay is 50%. For T_s between 0.1 and 0.4°C, these data contribute to an estimate for *b* of 0.20–0.41 m·a$^{-1/2}$, as outlined in Table 3. Since the mean annual ground temperature at 1 m is 0.7°C, and at 1.5 m is 0.1°C, the agreement between observed (Fig. 18) and calculated (Table 3) values for *b* verifies the application of [7] to thawing of permafrost at the burned site in general terms. Table 3 also indicates the sensitivity of *b* to variation in the ground ice content below, and moisture content above, the permafrost table. Such variations may account for the degradation of permafrost to 4.5 m by 1982, as reported above from other sites in the burned area. Furthermore, [8] takes no account of consolidation. The presence of excess ice will tend to reduce any empirically determined value for *b*, because the thickness of ground thawed is greater than the resultant overlying sediments.

To consider the time required for eradication of permafrost at the burned site, we rearrange [8] to give

[11] $t = z^2/b^2$

If thawing of permafrost were to proceed only by conduction from the surface downwards, [11] suggests that over 1300 years would be required to thaw the 14 m of ice-rich permafrost originally at the site. Even if significant convective effects continue at the burned site, and only the uppermost 7 m are thawed from the top down, nearly 340 years are required. These results are not altered in order-of-magnitude terms by substitution of other values for *b*, as in Table 3, and demonstrate the persistence of relatively thin ice-rich permafrost, found near the southerly margins of the discontinuous permafrost zone. The data indicate the time scale involved in the response of permafrost to ground warming.

The response of permafrost to climate warming is a popular topic in discussions of the impact of an enhanced atmospheric greenhouse effect on Canada (e.g., Woo et al. 1992; Kwong and Gan 1994; Riseborough and Smith 1994). The data from Takhini indicate that in southern Yukon Territory, wholesale degradation of ice-rich permafrost would occur over a century or less only at sites where the perennially frozen ground is at most 4–5 m thick, unless there are additional convective, that is, groundwater, effects. Considerable deepening of the active layer may occur more quickly.

The Takhini sites are only a partial analogue for examination of the effects of climate warming on permafrost, because the disturbance to ground temperatures has been forced by a drastic change in surface conditions, while climate has been relatively constant. Permafrost degradation at the Takhini sites is likely to be arrested if vegetation succession and regrowth of forest species occur over the next century, as indicated by the occurrence of ground ice between 2.0 and 2.8 m in the moist area drilled in 1982 (Fig. 2*b*).

Conclusions

From the data and analyses presented above we conclude the following:

(1) At a burned site studied in detail, the change in surface conditions effected by the 1958 Takhini Valley fire had led to 2.4 m of permafrost degradation by 1997, and ground temperatures throughout permafrost had been warmed to ≥–0.2°C.

(2) Equilibrium mean annual near-surface ground temperatures at sites in the valley with and without permafrost are approximately –0.8°C and 2.0°C, respectively. At burned sites, near-surface ground temperatures are transitional between these states.

(3) The active layer at the undisturbed forest site is 1.4 m thick, while 38 years after the fire (1996), the active layer at the burned site was 3.8 m thick. No residual thaw layer has been recorded at the burned site.

(4) The degradation of the upper surface of permafrost conforms to a conductive heat transfer regime in fine-grained surficial sediments, but convection appears responsible for permafrost degradation at the base of permafrost, with heat supplied from below.

(5) Over a millennium would be required for complete degradation of permafrost under the present ground thermal regime in the burned area. However, vegetation succession will likely arrest permafrost degradation over the next century, ceteris paribus.

(6) The time scale for eradication of relatively thin permafrost following natural disturbance, and, likely, climate warming, is on the order of centuries and millennia. Ground instability associated with active-layer deepening may occur in less than a decade.

(7) The *n*-factors used to summarize relations between air and near-surface ground temperatures are relatively well constrained for data collected in summer, when linear relations describe the correlation between these variables. In winter, the ground temperature at a depth of 20 cm is sensitive to heat stored lower in the profile and to the insulating effect of snow cover, and does not vary daily with air temperature in a clear fashion.

Acknowledgments

This paper is dedicated to the memory of Stephen C. Zoltai, out of respect for his inspirational research on permafrost response to forest fire. The Natural Sciences and Engineering Research Council of Canada, the Earth Physics Branch, Energy, Mines and Resources Canada, and Northern Research Endowment Fellowships from the Northern Research Institute, Yukon College, have supported the research. M.W. Smith, Carleton University, initiated the field programme. Reliable data collection by John Bunker, Scott Smith, Ann Macdonald, the late Gerald Hunter, Rob Hunter, Ross Carroll, and Diana and Karen White, all of Whitehorse, has made this research possible. Dan Riseborough, the late Mike Hare, Alan Dufour, Todd Randall, John Schilling, Carrie-Lynn Brown, Mark Carroll, Brenda Sproule, Michel Carron, and Brenda Adams assisted with drilling and laboratory work. Don Watt and David Millar, Yukon Weather Centre, have supplied weather data. Some samples were processed in the Soil Testing Laboratory, Public Works Canada (now Highways Engineering Branch, Yukon Territorial Government), by kind permission of Roy Lidgren and Doug Johnson. Complimentary work in N.W.T. has been supported by Rick Lanoville, Forest Management Division, Government of the Northwest Territories. The extent of fieldwork near Whitehorse would not have been possible without the encouragement of Joan Ramsay Burn and the hospitality of Desmond and Marion Carroll. Helpful background on the Takhini Valley fires of 1958 was provided by Keith Kepke. The sustained interest of Scott Smith, Charlotte Mougeot, Steve Morison, Charlie Roots, and Gary White, all of Whitehorse, is acknowledged with gratitude. The paper was written while on sabbatical leave as a Visiting Scientist at the Geological Survey of Canada. Helpful comments on the paper were received from J.R. Mackay, S.I. Outcalt, M.W. Smith, D.K. Swanson, and a referee.

References

Andersland, O.B., and Ladanyi, B. 1994. An introduction to frozen ground engineering. Chapman and Hall, New York, N.Y.

Burgess, M.M., Judge, A.S., and Taylor, A.E. 1982. Yukon ground temperature data collection—1966 to August 1981. Energy, Mines and Resources Canada, Earth Physics Branch, Open File 82-1.

Burn, C.R. 1987. Thermokarst ponds and ground temperatures in Takhini Valley. *In* XIIth INQUA Congress field excursions A20 and A20*b* Research in Yukon. *Edited by* S.R. Morison and C.A.S. Smith. National Research Council of Canada, Ottawa, Ont., p. 34.

Burn, C.R. 1992. Recent ground warming inferred from the temperature in permafrost near Mayo, Yukon Territory. *In* Periglacial geomorphology. *Edited by* J.C. Dixon and A.D. Abrahams. Proceedings, 22nd Binghampton Symposium on Geomorphology, John Wiley and Sons Ltd. New York, N.Y., pp. 327–350.

Burn, C.R. 1997. Cryostratigraphy, paleogeography, and climate change during the early Holocene warm interval, western Arctic coast, Canada. Canadian Journal of Earth Sciences, **34**: 912–925.

Burn, C.R., and Smith, C.A.S. 1988. Observations of the "thermal offset" in near-surface mean annual ground temperatures at several sites near Mayo, Yukon Territory, Canada. Arctic, **41**: 99–104.

Burn. C.R., and Smith, M.W. 1990. Development of thermokarst lakes during the Holocene at sites near Mayo, Yukon Territory. Permafrost and Periglacial Processes, **1**: 161–176.

Cheng, G. 1983. The mechanism of repeated-segregation for the formation of thick-layered ground ice. Cold Regions Science and Technology, **8**: 57–66.

Environment Canada. 1993. Canadian climate normals, 1961–90, Yukon and Northwest Territories. Environment Canada, Canadian Climate Program.

Flannigan, M.D., and Van Wagner, C.E. 1991. Climate change and wildfire in Canada. Canadian Journal of Forest Research, **21**: 66–72.

Harris, S.A., French, H.M., Heginbottom, J.A., Johnston, G.H., Ladanyi, B., Sego, D.C., and van Everdingen, R.O. 1988. Glossary of permafrost and related ground-ice terms. National Research Council of Canada, Technical Memorandum 142.

Heginbottom, J.A. 1995. Canada—Permafrost. *In* National atlas of

Canada. 5th ed. Natural Resources Canada, Ottawa., Ont., Plate 2.1, MCR 4177.

Hinkel, K.M., Outcalt, S.I., and Taylor, A.E. 1997. Seasonal patterns of coupled flow in the active layer at three sites in northwest North America. Canadian Journal of Earth Sciences, **34**: 667–678.

Hughes, O.L., Rutter, N.W., and Clague, J.J. 1989. Yukon Territory (Quaternary stratigraphy and history, Cordilleran Ice Sheet). *In* Quaternary geology of Canada and Greenland. *Edited by* R.J. Fulton. Geological Survey of Canada, Geology of Canada, Vol. 1, pp. 58–67.

Johansen, Ø. 1975. Thermal conductivity of soils. Ph.D. thesis, Norwegian Technical University, Trondheim. (In Norwegian.) *Translated in* U.S. Army, Cold Regions Research and Engineering Laboratory, Translation 637.

Jorgenson, M.T., and Kreig, R.A. 1988. A model for mapping permafrost distribution based on landscape component maps and climatic variables. *In* Proceedings, 5th International Conference on Permafrost, Trondheim, Norway, August 2–5, 1988. Tapir Publishers, Trondheim, Norway, Vol. 1, pp. 176–182.

Keenan, T.J., and Cwynar, L.C. 1992. Late Quaternary history of black spruce and grasslands in southwest Yukon Territory. Canadian Journal of Botany, **70**: 1336–1345.

Klassen, R.W. 1979. Thermokarst terrain near Whitehorse, Yukon Territory. *In* Current research, part A. Geological Survey of Canada, Paper 79-1A, pp. 385–388.

Kwong, Y.T.J., and Gan, T.Y. 1994. Northward migration of permafrost along the Mackenzie Highway and climatic warming. Climatic Change, **26**: 399–419.

Lunardini, V.J. 1978. Theory of *n*-factors and correlation of data. *In* Proceedings, 3rd International Conference on Permafrost, Edmonton, Alta, July 10–13, 1978. National Research Council of Canada, Ottawa, Ont., Vol. 1, pp. 40–46.

Mackay, J.R. 1977. Changes in the active layer from 1968 to 1976 as a result of the Inuvik fire. *In* Report of activities, part B. Geological Survey of Canada, Paper 77-1B, pp. 273–275.

Mackay, J.R. 1983. Downward water movement into frozen ground, western Arctic coast, Canada. Canadian Journal of Earth Sciences, **20**: 120–134.

Mackay, J.R. 1995. Active layer changes (1968 to 1993) following the forest–tundra fire near Inuvik, N.W.T., Canada. Arctic and Alpine Research, **27**: 323–336.

Mark, D.M., and Church, M. 1977. On the misuse of regression in earth science. Mathematical Geology, **9**: 63–75.

Mathews, W.H. 1986. Physiography of the Canadian Cordillera. Geological Survey of Canada, Map 1701A.

Moore, P.D. 1996. Fire damage soils our forests. Nature (London), **384**: 312–313.

Morison, S.R., and Klassen, R.W. 1991. Surficial geology, Whitehorse, Yukon Territory. Geological Survey of Canada, Map 12-1990.

Muller, S.W. 1947. Permafrost or permanently frozen ground and related engineering problems. J.W. Edwards, Ann Arbor, Mich.

Murton, J.B., and French, H.M. 1993. Thermokarst involutions, Summer Island, Pleistocene Mackenzie Delta, western Canadian Arctic. Permafrost and Periglacial Processes, **4**: 217–229.

Murton, J.B., Whiteman, C.A., and Allen, P. 1995. Involutions in the Middle Pleistocene (Anglian) Barham Soil, eastern England: a comparison with thermokarst involutions from arctic Canada. Boreas, **24**: 269–280.

Patterson, D.E., and Smith, M.W. 1981. The measurement of unfrozen water content by time domain reflectometry: results from laboratory tests. Canadian Geotechnical Journal, **18**: 131–144.

Rampton, V.N., Ellwood, J.R., and Thomas, R.D. 1983. Distribution and geology of ground ice along the Yukon portion of the Alaska Highway gas pipeline. *In* Proceedings, 4th International Conference on Permafrost, Fairbanks, Alaska, July 17–22, 1983. National Academy Press, Washington, D.C., Vol. 1, pp. 1030–1035.

Riseborough, D.W. 1990. Soil latent heat as a filter of the climate signal in permafrost. *In* Proceedings, 5th Canadian Permafrost Conference, Québec, Que., June 6–10, 1990. Centre d'études nordiques, Université Laval, Québec, pp. 199–205.

Riseborough, D.W., and Smith, M.W. 1994. Modelling permafrost response to climate change and climate variability. *In* Proceedings, 4th International Symposium on Thermal Engineering and Science for Cold Regions, Hanover, N.H., September 28 – October 1, 1993. *Edited by* V.J. Lunardini and S.L. Bowen. U.S. Army, Cold Regions Research and Engineering Laboratory, Hanover, N.H., pp. 179–187.

Romanovsky, V.E., and Osterkamp, T.E. 1997. Thawing of the active layer on the coastal plain of the Alaskan Arctic. Permafrost and Periglacial Processes, **8**: 1–22.

Rouse, W.R. 1976. Microclimatic changes accompanying burning in subarctic lichen woodland. Arctic and Alpine Research, **8**: 357–376.

Smith, M.W. 1975. Microclimatic influences on ground temperatures and permafrost distribution, Mackenzie Delta, Northwest Territories. Canadian Journal of Earth Sciences, **12**: 1421–1438.

Smith, M.W., and Riseborough, D.W. 1983. Permafrost sensitivity to climatic change. *In* Proceedings, 4th International Conference on Permafrost, Fairbanks, Alaska, July 17–22, 1983. National Academy Press, Washington, D.C., Vol. 1, pp. 1178–1183.

Swanson, D.K. 1996. Susceptibility of permafrost soils to deep thaw after forest fires in interior Alaska, U.S.A., and some ecologic implications. Arctic and Alpine Research, **28**: 217–227.

Taylor, A.E. 1995. Field measurements of *n*-factors for natural forest areas, Mackenzie Valley, Northwest Territories. Geological Survey of Canada, Current Research 1995-B, pp. 89–98.

Viereck, L.A. 1973. Ecological effects of river flooding and forest fires on permafrost on the taiga of Alaska. *In* North American Contribution, 2nd International Conference on Permafrost, Yakutsk, U.S.S.R., July 13–28, 1973. National Academy of Sciences, Washington, D.C., pp. 60–67.

Viereck, L.A. 1982. Effects of fire and firelines on active layer thickness and soil temperatures in interior Alaska. *In* Proceedings, 4th Canadian Permafrost Conference, Calgary, Alta., March 2–6, 1980. *Edited by* H.M. French. National Research Council of Canada, Ottawa, Ont., pp. 123–135.

Wahl, H.E., Fraser, D.B., Harvey, R.C., and Maxwell, J.B. 1987. Climate of Yukon. Environment Canada, Atmospheric Environment Service, Climatological Studies 40.

Williams, D.J., and Burn, C.R. 1996. Surficial characteristics associated with the occurrence of permafrost near Mayo, central Yukon Territory, Canada. Permafrost and Periglacial Processes, **7**: 193–206.

Woo, M.-k., Lewkowicz, A.G., and Rouse, W.R. 1992. Response of the Canadian permafrost environment to climatic change. Physical Geography, **13**: 287–317.

Zhou, Y., Liang, L., Gu, Z., Liang, F., and Zhang, Q. 1993. Effects of forest fire on the hydro-thermal regime of frozen ground, the northern part of Da Hinggan Ling, China. *In* Proceedings, 6th International Conference on Permafrost, Beijing, China, July 5–9, 1993. South China University of Technology Press, Wushan Guangzhou, China, pp. 819–825.

Zoltai, S.C. 1993. Cyclic development of permafrost in the peatlands of northwestern Alberta, Canada. Arctic and Alpine Research, **25**: 240–246.